Nonmonotonic effects of perpendicular magnetic anisotropy on current-driven vortex wall motions in magnetic nanostripes*

Su Yuan-Chang(苏垣昌)†, Lei Hai-Yang(雷海洋), and Hu Jing-Guo(胡经国)‡

College of Physics Science and Technology, Yangzhou University, Yangzhou 225002, China

(Received 6 February 2015; revised manuscript received 1 April 2015; published online 21 July 2015)

In a magnetic nanostripe, the effects of perpendicular magnetic anisotropy (PMA) on the current-driven horizontal motion of vortex wall along the stripe and the vertical motion of the vortex core are studied by micromagnetic simulations. The results show that the horizontal and vertical motion can generally be monotonously enhanced by PMA. However, when the current is small, a nonmonotonic phenomenon for the horizontal motion is found. Namely, the velocity of the horizontal motion firstly decreases and then increases with the increase of the PMA. We find that the reason for this is that the PMA can firstly increase and then decrease the confining force induced by the confining potential energy. In addition, the PMA always enhances the driving force induced by the current.

Keywords: domain wall motion, current, perpendicular magnetic anisotropy, micromagnetic simulation

PACS: 75.60.Ch, 72.25.Pn, 75.78.Cd **DOI:** 10.1088/1674-1056/24/9/097506

1. Introduction

Current-induced domain wall (DW) motion in a magnetic nanostripe, which has potential applications to the next-generation data storage and logic devices, has been intensively studied in recent years.[1–5] For practical applications, how to enhance the DW motion with small current is an important concern. Thin stripes with high perpendicular magnetic anisotropy (PMA) have attracted much intention because they provide a pathway to lower the operation current against Joule heating effects.[3,6] It was reported that the current-driven motion of the transverse wall (TW) can be enhanced by tuning the PMA.[7] However, there is some confusion about the effects of PMA on the current-driven DW motion. The enhancement of domain wall (DM) motion may come from the decrease of the confining force induced by the confining potential energy[8,9] or the increase of the driving force induced by the current. However, how the PMA affects the confining force and the driving force has not been reported before.

In a magnetic nanostripe system, the vortex wall (VW) is one of the basic domain walls.[10–12] As for the VW, the current-driven motions are more complex than that of the TW, because the horizontal motion of VW along the stripe is accompanied by the vertical motion of the vortex core.[13] Theoretically, the study on the current-driven motions of the VW may clarify more of the underlying physical origins than that of the TW. Moreover, the vertical motion of the vortex core is important because it may affect the coupling between the VWs in two-stripe or two-VW systems.[14–18] Hence, it is necessary to clarify how the PMA affects the current-driven motions of the VW.

In this paper, the current-driven VW motions in magnetic nanostripe system with PMA are studied by Landau–Lifshitz–Gilbert (LLG) spin dynamics simulation. The numerical results show that the driving forces for both the horizontal motion and the vertical motion can be monotonously enhanced by the PMA and the current. However, the confining force induced by the confining potential energy firstly increases and then decreases with the increase of the PMA. As a result, the velocity of the horizontal motion firstly decreases and then increases with the increase of the PMA when the current is small. However, the velocity of the horizontal motion just increases as the PMA increases when the current is larger than a critical value. On the other hand, the velocity of the vertical motion increases with the PMA in a monotonous way. The underlying physical origins for these effects are quantitatively provided.

2. Model

The sample used in this paper has a width of 64 nm, a thickness of 10 nm, and a length of 2048 nm. This stripe is placed in x–y plane. The horizontal axis, the vertical axis, and the perpendicular axis are defined as x axis, y axis, and z axis, respectively. In simulations, the unit cell size $a \times a \times b$ is 4 nm $\times$ 4 nm $\times$ 10 nm. The saturation magnetization $M_s = 1.4 \times 10^6$ A/m, and the exchange stiffness $A = 2.0 \times 10^{-11}$ J/m.[19] In the initial state, a VW is placed in the center of the stripe by the helping of the mathematical equation given in Ref. [20]. In order to minimize the ef-

*Project supported by the National Natural Science Foundation of China (Grant Nos. 11247026 and 11374253).

†Corresponding author. E-mail: ycsu@yzu.edu.cn

‡Corresponding author. E-mail: jghu@yzu.edu.cn

© 2015 Chinese Physical Society and IOP Publishing Ltd

fects that appear when DW approaches the end of the stripe, a scheme that keeps the VW centered in the computational region[21–23] has been used. It shows this magnetic structure is a stable configuration even though the VW is not the ground state of the investigated system. As shown in Fig. 1, when the PMA constant $K_z < 200$ kJ/m^3, the VW is a metastable state and can keep its shape under the spin transfer torque induced by spin-polarized current. When $K_z > 200$ kJ/m^3, the VW cannot be stable, namely the stable state only favors a TW.

The model's Hamiltonian is

$$H = -J_{\rm ex}\sum_{\langle i,j\rangle} \boldsymbol{M}_i\cdot\boldsymbol{M}_j - \sum_i K^z(M_i^z)^2 - g\mu_{\rm B}\sum_i \boldsymbol{h}\cdot\boldsymbol{M}_i + \frac{\omega}{2}\sum_{i\neq j}\left[\frac{\boldsymbol{M}_i\cdot\boldsymbol{M}_j}{r_{ij}^3} - 3\frac{(\boldsymbol{r}_{ij}\cdot\boldsymbol{M}_i)(\boldsymbol{r}_{ij}\cdot\boldsymbol{M}_j)}{r_{ij}^5}\right], \quad (1)$$

where $\boldsymbol{M}_i$ and $\boldsymbol{M}_j$ are the unit magnetizations for unit cells i and j. The $J_{\rm ex}$ is the exchange coupling constant for the nearest neighbor cells. The K^z is the perpendicular anisotropy constant. The third term is Zemman energy, and g, $\mu_{\rm B}$, and h denote Lande factor, Bohr magneton, and the external field, respectively. The $\boldsymbol{r}_{ij}$ denotes the lattice vector between cells i and j. The ω is the dipole–dipole coupling parameter. Here, only the dipolar interaction is contained. The sizeable contribution for adjacent cells, namely all higher orders of the multipole expansion, are neglected. Parameters $J_{\rm ex}$ and ω can be obtained by $J_{\rm ex} = Aa$ and $\omega = \frac{\mu_0}{4\pi}MS^2V_{\rm cell}$,[24,25] where $V_{\rm cell} = a^2b$.

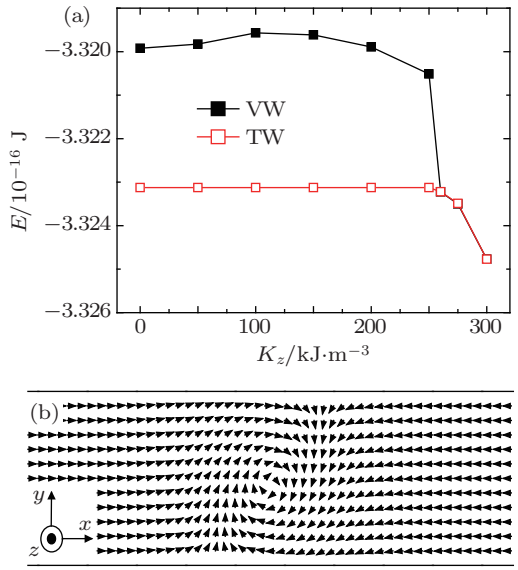


Fig. 1. (color online) (a) Energies of VW system and TW system as a function of PMA. (b) The stable initial state with a VW in the center of the stripe.

When the current u is applied along the $+x$ direction, the generalized LLG equation with additional adiabatic and nonadiabatic spin-transfer torque[26–28] can be written as

$$\frac{\partial \boldsymbol{M}}{\partial t} = -\gamma\boldsymbol{M}\times\boldsymbol{H}_{\rm eff} + \alpha\boldsymbol{M}\times\frac{\partial\boldsymbol{M}}{\partial t} + u\boldsymbol{M}\times\left(\boldsymbol{M}\times\frac{\partial\boldsymbol{M}}{\partial x}\right) + \beta u\boldsymbol{M}\times\frac{\partial\boldsymbol{M}}{\partial x}, \quad (2)$$

where $\boldsymbol{M}$ is the unit magnetization vector, $\boldsymbol{H}_{\rm eff}$ is the effective field including the anisotropy field, the magnetostatic field, and the exchange coupling field, γ is the gyromagnetic ratio, α is the Gilbert damping constant, β denotes the nonadiabatic spin torque coefficient, u is the effective drift velocity of the conduction electron spins defined by $u = {\rm j}Pg\mu_{\rm B}/2eM_{\rm s}$, with P being the spin polarization, j the current density, g the Lande factor, $\mu_{\rm B}$ the Bohr magneton, and e the carrier charge, respectively. In this paper, we choose $\alpha = 0.01$ and $\gamma = 2.21\times10^5$ m/As.[29] As for the VW, the non-adiabaticity parameter is found to be much larger than the damping constant α.[30,31] Therefore, $\beta = 0.05$ is assumed.

3. Results and discussion

Figure 2 shows the horizontal displacements d_x of the VW and the vertical displacements d_y of the vortex core as a function of simulation time with different currents. As the current increases, both the horizontal motion and the vertical motion are enhanced. This happens because both the third term and the fourth term in Eq. (2) increase with the current. As shown in Fig. 2, when the current is sufficiently small, e.g., $u = 35.2$ m/s, the vortex core moves a small distance in a vertical direction and then stops. This happens because a restoring force produced by two distorted TWs to the vortex core may prevent the vertical motion and keep the vortex core inside the stripe.[28,32,33] When the current is larger than a critical value (about 48 m/s), the restoring force is not able to prevent the vortex core bumping over the vertical boundary. In this case, the VW transforms to a TW when the vortex core moves out of the vertical boundary. These results agree well with the previous reports.[20,34]

Figure 3 shows the horizontal displacements d_x of the VW and the vertical displacements d_y of the vortex core as a function of simulation time with different PMA. It shows that the PMA has sizeable effects on both the horizontal motion and the vertical motion. The inset of Fig. 3(a) shows that as K_z increases, the time-averaged velocity V_x of the horizontal motion first decreases and then increases. This nonmonotonic effect has not been reported before and will be interpreted below. However, as shown in the inset of Fig. 3(b), the time-averaged velocity V_y of the vertical motion increases with K_z in a monotonous way. This monotonous effect comes from the fact that the fourth (precession) term in Eq. (2) can be enhanced by the PMA, which will also be discussed below.

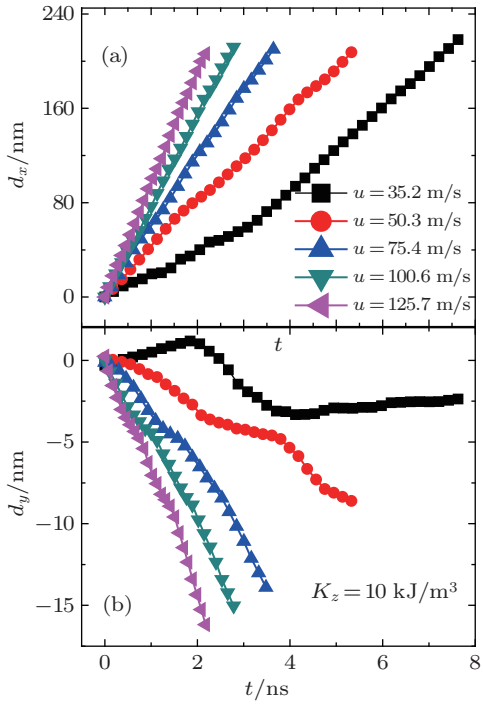


Fig. 2. (color online) (a) Horizontal displacements d_x of the VW and (b) vertical displacements d_y of the vortex core versus simulation time t with different currents. The PMA constant $K_z = 10$ kJ/m^3.

In order to understand the nonmonotonic effect of the PMA on the horizontal motion, the confining potential energy of the VW is calculated. The confining potential energy can be obtained by $E = E_{\text{demag}} + E_{\text{K}} + E_{\text{ex}}$, where E_{demag} is the demagnetization energy, E_{K} the anisotropic energy, and E_{ex} the exchange coupling energy of the system, respectively.

Figure 4 shows E, E_{demag}, E_{K}, and E_{ex} as a function of the horizontal positions x of the VW. Here, $x = 0$ denotes the center of the stripe. The energies (E_{demag}, E_{K}, and E_{ex}) are in value relative to E_{K} of $x = 0$. As shown in Fig. 4(a), firstly,

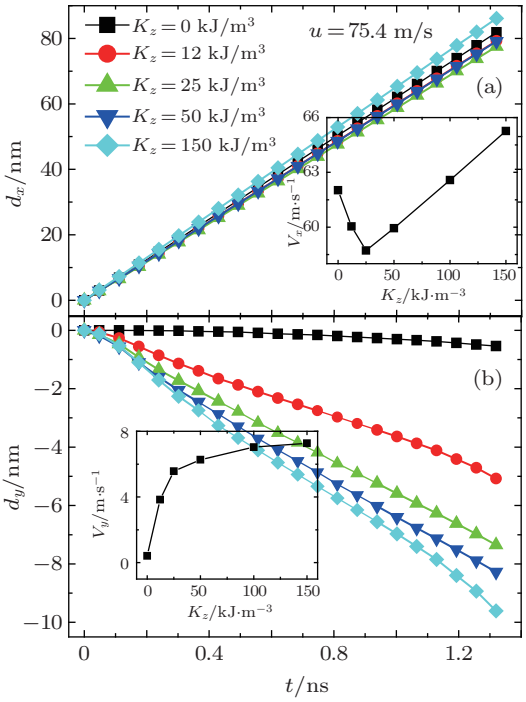


Fig. 3. (color online) (a) Horizontal displacements d_x of the VW and (b) vertical displacements d_y of the vortex core versus simulation time t with different PMA. The insets of panels (a) and (b) show the time-averaged velocities (within the range of 0–1.3 ns) of the horizontal motion and the vertical motion as a function of K_z, respectively. Parameter $u = 75.4$ m/s.

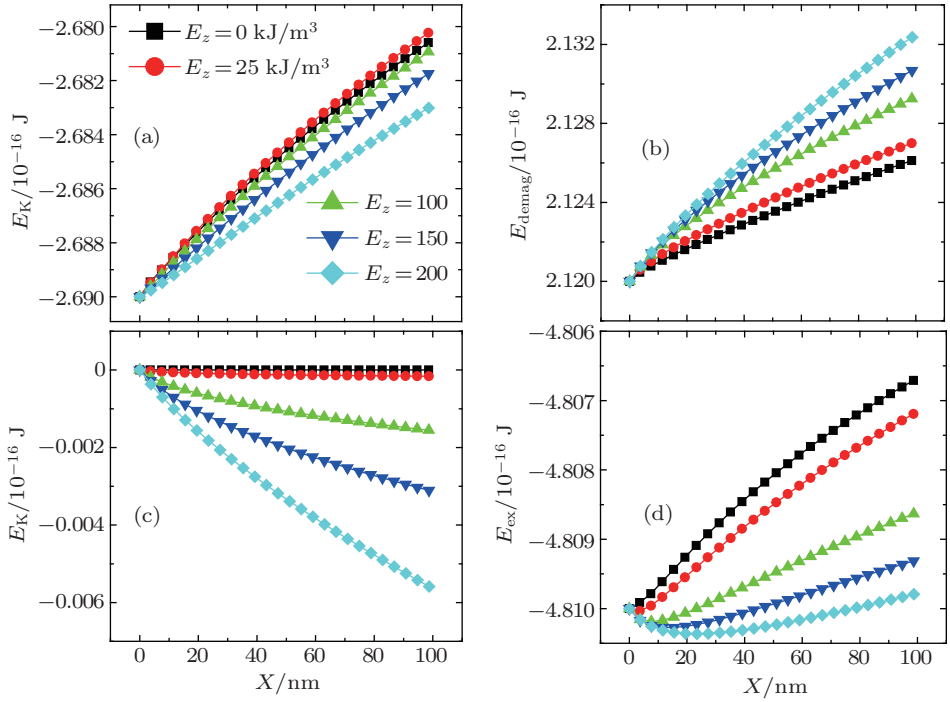


Fig. 4. (color online) (a) Confining potential energy E of the VW, (b) demagnetization energy E_{demag}, (c) anisotropic energy E_{K}, and (d) exchange coupling energy E_{ex} of the system versus horizontal positions x of the VW with different PMA. The $x = 0$ denotes the center of the stripe.

E increases as x increases, which leads to a confining force $F = -\partial E/\partial x$ for hindering the horizontal motion. Secondly, E increases with K_z when $K_z < 25$ J/m^3; when $K_z > 25$ J/m^3, E decreases with increasing K_z. It indicates that the confining force firstly increases, and then decreases with increasing K_z, which leads to the nonmonotonic effect of the PMA on the horizontal motion. In detail, as shown in Figs. 4(b)–4(d), it is found that $E_{\rm demag}$ increases with K_z, while $E_{\rm K}$ and $E_{\rm ex}$ decrease as K_z increases, so the confining potential energy E can increase firstly, and then decreases with increasing K_z. Here, some underlying physical origins should be illuminated: (i) as K_z increases, the z-component magnetic moment of each cell increases, which leads to the increase of $E_{\rm demag}$ and the decrease of $E_{\rm K}$; (ii) as the z-component magnetic moment of each cell increases, the angle between the magnetic moments of the adjacent cells decreases, which leads to the decrease of $E_{\rm ex}$; (iii) as x increases, $E_{\rm demag}$ and $E_{\rm ex}$ increase, which mainly comes from the magnetostatic confining effect of the stripe and the distortion of the VW shape.[18]

Interestingly, the effect of the PMA on the horizontal motion can be changed by tuning the current. Figure 5 shows the average velocity V_x of the horizontal motion as a function of K_z with different current. When $u < 100$ m/s, the function is nonmonotonic. When $u > 100$ m/s, the function becomes monotonous. This can be attributed to the PMA-induced competition between the confining force and the driving force for the horizontal motion. On the one hand, the PMA provides a nonmonotonic effect on the confining force, as mentioned above. On the other hand, the driving force for the horizontal motion always increases with both the PMA and the current, which is discussed below.

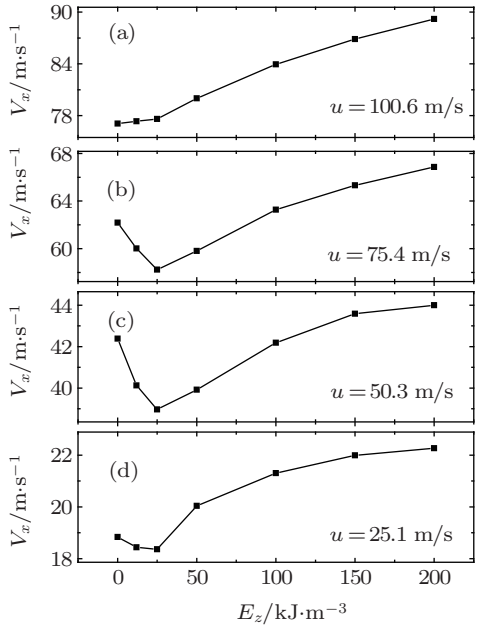


Fig. 5. The average velocity of the horizontal motion as a function of K_z with different current.

For convenience, equation (2) can be transformed into a more manageable equation, as denoted in Ref. [25], it is

$$\begin{aligned}\frac{\partial \boldsymbol{M}}{\partial t} &= -\frac{\gamma}{1+\alpha^2}\boldsymbol{M}\times\boldsymbol{H}_{\rm eff} - \frac{\gamma\alpha}{1+\alpha^2}\boldsymbol{M}\times(\boldsymbol{M}\times\boldsymbol{H}_{\rm eff}) \\ &\quad + \frac{(1+\alpha\beta)u}{1+\alpha^2}\boldsymbol{M}\times\left(\boldsymbol{M}\times\frac{\partial \boldsymbol{M}}{\partial x}\right) \\ &\quad - \frac{(\alpha-\beta)u}{1+\alpha^2}\boldsymbol{M}\times\frac{\partial \boldsymbol{M}}{\partial x}. \end{aligned} \tag{3}$$

The first term and the fourth term in Eq. (2) are precession terms. The second term and the third term are relaxation terms. In this way, the origins of the current-driven VW motions can be more easily understood. We have done some simulation by Eq. (2). The results show that the horizontal motion of VW is caused by the third (relaxation) term, while the vertical motion of the vortex core can be caused individually by the first (precession) and the fourth (precession) term. Hence, the driving forces induced by current for both the horizontal motion and the vertical motion is proportional to current u and the magnetization gradient $\partial \boldsymbol{M}/\partial x$.

In fact, the PMA can affect the driving forces for both the horizontal motion and the vertical motion due to the fact that the PMA may change the magnetization gradient of the system. For any horizontal position, the magnitude of the magnetization gradient can be defined as

$$\frac{\partial M}{\partial x} = \sqrt{\left(\frac{\partial M_x}{\partial x}\right)^2 + \left(\frac{\partial M_y}{\partial x}\right)^2 + \left(\frac{\partial M_z}{\partial x}\right)^2},$$

where M_x, M_y, and M_z denote the components of the magnetization moment at position x.

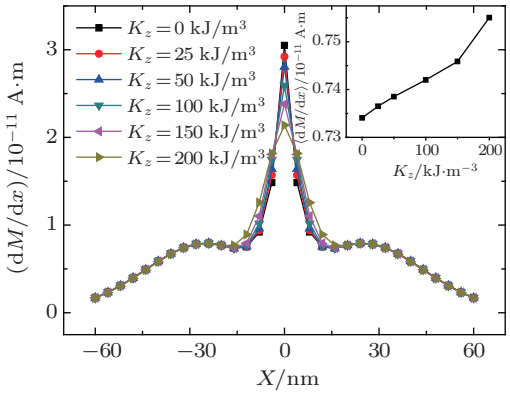


Fig. 6. (color online) The magnitude of the magnetization gradient $\partial M/\partial x$ of the initial state versus x with different K_z. The inset shows the average $\partial M/\partial x$ over the area of the VW (from $x = -60$ nm to $x = 60$ nm) versus K_z. $x = 0$ denotes the center of the stripe.

Figure 6 shows the magnitude of the magnetization gradient $\partial M/\partial x$ of the initial state as a function of x with different K_z. Here, M has been averaged in the y direction. When $x < -20$ nm or $x > 20$ nm, $\partial M/\partial x$ is almost independent of the K_z. When -20 nm $< x < -4$ nm or 4 nm

$< x <$ 20 nm, $\partial M/\partial x$ increases as K_z increases. At the position of the vortex core ($x = 0$), $\partial M/\partial x$ decreases as K_z increases. Importantly, the average $\partial M/\partial x$ in the range of the VW (from $x = -60$ nm to $x = 60$ nm) increases with K_z in a monotonous way, as shown in the inset of Fig. (6). Therefore, both the third (relaxation) term and the fourth (precession) term in Eq. (3) monotonously increase with the PMA, namely, the driving forces for both the horizontal motion and the vertical motion monotonously increase with the PMA. The fact that the driving force for the horizontal motion always increases with both the PMA and the current leads to the nonmonotonic effect of the PMA on the horizontal motion being erased by large current. In addition, the PMA monotonously enhances the driving force for the vertical motion leads to the monotonous effect of the PMA on the vertical motion of the vortex core.

4. Conclusions

In conclusion, both the confining force and the driving force can be affected by the PMA of the system. On the one hand, with the increase of the PMA, the confining potential energy first increases and then decreases, which leads to a nonmonotonic change of the confining force. On the other hand, the PMA can monotonously enhance the average magnetization gradient in the range of the VW, which leads to a monotonous enhancement of the driving force for both the horizontal motion and the vertical motion. Due to the PMA-induced competition between the confining force and the driving force for the horizontal motion, a nonmonotonic effect of the PMA on the horizontal motion occurs when the current is small, and the nonmonotonic effect is erased by a large current. Due to the PMA-induced enhancement of the driving force for the vertical motion, the vertical velocity of the vortex core monotonously increases with the PMA.

References

[1] Parkin S S P, Hayashi M and Thomas L 2008 *Science* **320** 190
[2] Boulle O, Malinowski G and Klaui M 2011 *Mater. Sci. Eng. R.* **72** 159
[3] Martinez E 2012 *J. Appl. Phys.* **111** 07D302
[4] Ryu J, Lee K J and Lee H W 2013 *Appl. Phys. Lett.* **102** 172404
[5] Fan Z, Ma X P, Lee S H, Shim J H, Piao H G and Kim D H 2012 *Acta Phys. Sin.* **61** 107502 (in Chinese)
[6] Kim K J, Lee J C, Yun S J, Gim G H, Lee K S, Choe S B and Shin K H 2010 *Appl. Phys. Express* **3** 083001
[7] Emori S and Beach G S D 2011 *Appl. Phys. Lett.* **98** 132508
[8] Bedau D, Kläui M, Hua M T, Krzyk S, Rüdiger U, Faini G and Vila L 2008 *Phys. Rev. Lett.* **101** 256602
[9] Hayashi M, Thomas L, Rettner C, Moriya R and Parkina S S P 2008 *Appl. Phys. Lett.* **92** 162503
[10] McMichael R D and Donahue M J 1997 *IEEE. Trans. Magn.* **33** 4167
[11] Nakatani Y, Thiaville A and Miltat J 2005 *J. Magn. Magn. Mater.* **290** 750
[12] Wang Y, Su Y and Hu J 2013 *J. Magn. Magn. Mater.* **328** 21
[13] Kim S, Lee K, Kim W and Lee T 2007 *Appl. Phys. Lett.* **90** 252508
[14] Laufenberg M, Bedau D, Ehrke H, Kläui M, Rüdiger U, Backes D, Heyderman L J, Nolting F, Vaz C A F, Bland J A C, Kasama T, Dunin-Borkowski R E, Cherifi S, Locatelli A and Heun S 2006 *Appl. Phys. Lett.* **88** 212510
[15] Hayward T J, Bryan M T, Fry P W, Fundi P M, Gibbs M R J, Allwood D A, Im M Y and Fischer P 2010 *Phys. Rev. B* **81** 020410(R)
[16] Hayward T J, Bryan M T, Fry P W, Fundi P M, Gibbs M R J, Im M Y, Fischer P and Allwood D A 2010 *Appl. Phys. Lett.* **96** 052502
[17] O'Brien L, Lewis E R, Fernández-Pacheco A, Petit D, Cowburn R P, Sampaio J and Read D E 2012 *Phys. Rev. Lett.* **108** 187202
[18] Su Y, Sun J, Hu J and Lei H 2013 *Europhys. Lett.* **103** 67004
[19] Lin C, Gorman G, Lee C, Farrow R, Marinero E, Do H, Notarys H and Chien C 1991 *J. Magn. Magn. Mater.* **93** 194
[20] He J, Li Z and Zhang S 2006 *Phys. Rev. B* **73** 184408
[21] Nakatani Y, Thiaville A and Miltat J 2003 *Nat. Mater.* **2** 521
[22] Martinez E, Lopez-Diaz L, Torres L, Tristan C and Alejos O 2007 *Phys. Rev. B* **75** 174409
[23] Szambolics H, Toussaint J C, Marty A, Miron I M and Buda-Prejbeanu L D 2009 *J. Magn. Magn. Mater.* **321** 1912
[24] Schieback C, Kläui M, Nowak U, Rüdiger U and Nielaba P 2007 *Eur. Phys. J. B* **59** 429
[25] Wieser R, Vedmedenko E Y, Weinberger P and Wiesendanger R 2010 *Phys. Rev. B* **82** 144430
[26] Zhang S and Li Z 2004 *Phys. Rev. Lett.* **93** 127204
[27] Thiaville A, Nakatani Y, Miltat J and Suzuki Y 2005 *Europhys. Lett.* **69** 990
[28] Mougin A, Cormier M, Adam J P, Metaxas P J and Ferré J 2007 *Europhys. Lett.* **78** 57007
[29] Roy P E and Wunderlich J 2011 *Appl. Phys. Lett.* **99** 122504
[30] Heyne L, Rhensius J, Ilgaz D, Bisig A, Rüdiger U and Kläui M 2010 *Phys. Rev. Lett.* **105** 187203
[31] Eltschka M, Wötzel M, Rhensius J, Krzyk S, Nowak U and Kläui M 2010 *Phys. Rev. Lett.* **105** 056601
[32] Guslienko K Y, Ivanov B A, Novosad V, Otani Y, Shima H and Fukamichi K 2002 *J. Appl. Phys.* **91** 8037
[33] Guslienko K Y, Novosad V, Otani Y, Shima H and Fukamichi K 2001 *Appl. Phys. Lett.* **78** 3848
[34] He J, Li Z and Zhang S 2006 *J. Appl. Phys.* **99** 08G509